

Decon nement Phase Transition in 3D Nonlocal U(1) Lattice Gauge Theory

Gaku Arakawa and Ikuo Ichinose

Department of Applied Physics, Nagoya Institute of Technology, Nagoya, 466-8555 Japan

Tetsuo Matsui

Department of Physics, Kinki University, Higashi-Osaka, 577-8502 Japan

Kazuhiko Sakakibara

Department of Physics, Nara National College of Technology, Yamatokohriyama, 639-1080 Japan

(February 8, 2020)

We introduce a 3D compact U(1) lattice gauge theory having nonlocal interactions in the temporal direction, and study its phase structure. The model is relevant for the compact QED₃ and strongly correlated electron systems like the t-J model of cuprates. For a power-law decaying long-range interaction, which simulates the effect of gapless matter fields, a second-order phase transition takes place separating the con nement and decon nement phases. For an exponentially decaying interaction simulating gapful matter fields, the system exhibits no signals of a second-order transition.

11.15.-q, 71.27.+a

The U(1) lattice gauge theory (LGT) in three dimensions (3D) coupled to matter fields describes various interesting physical systems. The compact QED₃ is just a such system and its phase structure has been studied by various methods¹. In condensed matter physics, interesting observations were made that the strongly-correlated electron systems in two dimensions like the antiferromagnetic Heisenberg spin model, the t-J model of high-T_c cuprates, and the fractional quantum Hall states are described by 3D U(1) gauge theories due to the introduction of auxiliary collective fields^{2,5}.

For the case without matter-field couplings, Polyakov⁶ showed that the 3D compact U(1) gauge theory is always in the con nement phase due to the monopole (instanton) condensation. For the case with couplings to matter fields, there is still no consensus on the question of whether the system in two spatial dimensions exhibits a phase transition into a decon nement phase. Probably the answer depends on the properties of coupled matter fields. This question is important because the "fractionalization" of electrons may be interpreted as the decon nement phenomenon of U(1) gauge dynamics. For the t-J model, the possibility of charge-spin separation (CSS) is of great interest since it may explain various anomalous behaviors of the metallic state of cuprates⁷. In Ref.⁸ it was argued that the CSS takes place below certain critical temperature (T) as a decon nement (perturbative) phase of an effective U(1) LGT which is derived by the hopping expansion of spinons and holons in the slave-particle representation at finite T. In related works, Nagaosa⁹ argued that the decon nement phase is possible above some T, whereas Nayak¹⁰ argued that decon nement does not occur at any T. The decon nement phase at T = 0 for systems with gapless excitations are supported in Ref.¹¹ and denied in Ref.¹².

In this paper, we introduce and study a LGT with nonlocal interactions in order to investigate the phase structure of compact U(1) gauge theories coupled to matter

fields on the 3D lattice (2D system at T = 0). We first consider the cases of massless and massive relativistic matter fields. Then we apply the model to the nonrelativistic electron systems. The results of this paper for gapless excitations in electron systems shall complement our previous result of CSS⁸ because the hopping expansion employed there may be inadequate for massless excitations at T = 0.

Let us start with the path-integral representation of the partition function of gauge field U_x and (bosonic and/or fermionic) matter fields ψ_x ,

$$Z = \int \prod_{\mathbf{x}} d\psi_x d\bar{\psi}_x dU_x \exp(A);$$

$$A = \sum_{\mathbf{x}, \mathbf{y}} \psi_x \gamma_{xy}(U) \bar{\psi}_y + A_U;$$

$$A_U = q \sum_{\mathbf{x}; <} \prod_{\mathbf{x}; >} (U_x U_{x+\hat{\mu}}; U_{x+\hat{\mu}}; U_x + c.c.); \quad (1)$$

where $\mathbf{x} = (x_0; x_1; x_2)$ is the site-index of the 3D lattice of the size $V = N_0 N_1 N_2$ with the periodic boundary condition, $\hat{\mu} = (0; 1; 2)$ is the (imaginary) time and spatial direction index, ψ_x is the matter field on \mathbf{x} , $U_x = \exp(i\theta_x)$ ($\theta_x < 2\pi$) is the U(1) gauge variable on the link $(\mathbf{x}; \mathbf{x} + \hat{\mu})$, $\gamma_{xy}(U)$ represents the local couplings of ψ_x to U_x .

By integrating over ψ_x , we obtain an effective gauge theory,

$$Z = \int \prod_{\mathbf{x}} dU_x \exp \left[\sum_{\mathbf{x}} f \text{Tr} \log \gamma_{xy}(U) + A_U \right]; \quad (2)$$

where f is a parameter counting the statistics and internal degrees of freedom of ψ_x . Due to the $(\text{Tr} \log)$ term, the effective gauge theory becomes nonlocal. For relativistic matter fields, it is expanded as a sum over all the closed random walks R (loops including backtracks)

on the 3D lattice which represent world lines of particles and antiparticles as

$$\text{Tr} \log_{xy} (U) = \sum_R \frac{L[R]}{L[R]} \sum_{(x,y) \in R} U_x \quad (3)$$

$L[R]$ is the length of R , and $\kappa = (6 + m^2)^{-1}$ is the hopping parameter (6 is the number of links emanating from each site, and m is the mass of the matter field in unit of the lattice spacing). For the constant gauge field configuration $U_x = 1$, the expansion in (3) is logarithmically divergent $\sim \log m$ as $m \rightarrow 0$ due to the lowest-energy zero-momentum mode.

Below we shall study a slightly more tractable model than that given by Eq.(2). It is suggested from the formal hopping expansion (3), and obtained by retaining only the rectangular loops extending in the temporal direction in the loop sum and choosing their coefficients optimally as follows;

$$\begin{aligned} Z_T &= \int \prod_x dU_x \exp(A_T); \\ A_T &= g \sum_{x, i=1}^3 \sum_{\hat{y}} X^2 \tilde{X}^0 c (V_{x,ji} + V_{x,ji}) + A_S; \\ V_{x,ji} &= U_{x+\hat{0},j} \prod_{k=0}^{j-1} U_{x+\hat{1}+k\hat{0},0} U_{x+\hat{1}+k\hat{0},j} U_{x,i}; \\ A_S &= g \sum_x (U_{x,2} U_{x+\hat{2},1} U_{x+\hat{1},2} U_{x,1} + \text{c.c.}); \end{aligned} \quad (4)$$

$V_{x,ji}$ is the product of U_x along the rectangular $(x; x+\hat{1}; x+\hat{1}+\hat{0}; x+\hat{0})$ of size $(1, j)$ in the $(i, 0)$ plane. In A_S , we have retained only the nearest-neighbor spatial coupling. For the nonlocal coupling constant c , we consider the following two cases;

$$c = \begin{cases} \frac{1}{e^m}; & \text{power law decay (PD)}; \\ e^{-m}; & \text{exponential decay (ED)}; \end{cases} \quad (5)$$

The power 1 in the PD case in (5) reflects the effect of massless excitations. In fact, this c generates a logarithmically divergent action for $U_x = 1$ explained below Eq.(3) as one can see from the relation, $\exp(-m) \sim \log(1+m)$. The action for $m = 0$ is then proportional to $\log N_0$ for finite N_0 . On the other hand, the ED model contains m and simulates the case of massive matter fields¹³.

We made Monte Carlo simulations to determine the phase structure of this model. We consider the isotropic lattice, $N = N^3$, with the periodic boundary condition up to $N = 32$, where the limit $N \rightarrow \infty$ corresponds to the system on a 2D spatial lattice at $T = 0$. For the mass of the ED model, we set $m = 1$. For the spatial coupling scaled by g , we consider the two typical cases $\kappa = 0$ (i.e., no spatial coupling) and $\kappa = 1$.

First, we calculate the following average E ("internal energy") and the fluctuation C ("specific heat") of A_T ;

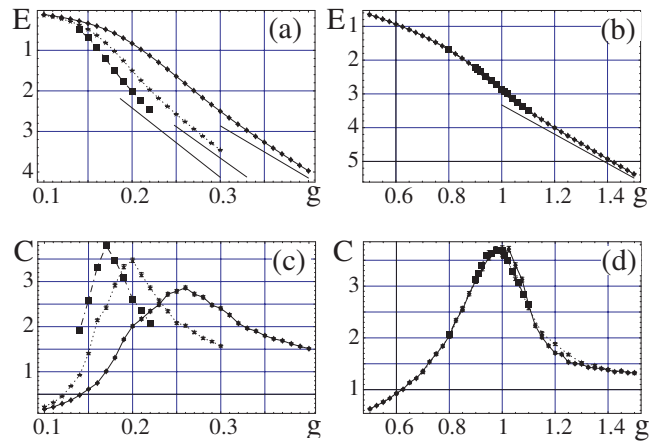


FIG. 1. Internal energy E and the fluctuation C of the action with $\kappa = 1$ vs non-local coupling g for $N = 8$ (a); 16 (b); 24 (c); (a,c) PD model, (b,d) ED model. The solid lines in (a) and (b) are the large- g expansion. In the PD model, strong N dependence is observed in E at large g and in the developing peak of C . They indicate a second-order phase transition in the PD model.

$$E = \langle A_T \rangle; \quad C = \langle (A_T - \langle A_T \rangle)^2 \rangle \quad (6)$$

For small g , the high-temperature expansion (HTE) gives $Z \sim \exp[g^2(2Q_2 + \kappa^2)V] (Q_k \sim c^k)$, whereas for large g , the low-temperature expansion (LTE) around $V_{x,ji} = 1$ gives $Z \sim \exp[(4gQ_1 + 2g \log g)V]$.

In Fig.1, we present $E; C$ for $\kappa = 1$ vs the nonlocal coupling g . They agree with the above HTE and LTE. In the PD model, E of Fig.1 (a) connects the HTE result and LTE result, showing that $V_{x,ji} \rightarrow 1$ for large g . C in Fig.1 (c) shows that its peak develops as N increases. These results indicate that the PD model exhibits a second-order phase transition separating the disordered (confinement) phase and the ordered (deconfinement) phase at $g = g_c \approx 0.17$, which is determined from the data of $N = 24$. This transition will be confirmed later by the measurement of Polyakov lines. On the other hand, the peak of C in the ED model does not develop as N increases, showing no signals of a second-order transition. It may have a higher-order transition or just a crossover. Simulations of the models with $\kappa = 0$ give similar behaviors of $E; C$, preserving the above phase structure for $\kappa = 1$.

To study the nature of gauge dynamics, we calculated the spatial correlations of Polyakov lines P_{x_2} ;

$$\begin{aligned} P_{x_2} &= \prod_{x_0=1}^{x_2} U_{x_2, x_0, 0}; \quad (x_2 = (x_1; x_2)); \\ f_P(x_2) &= \langle P_{x_2} P_{0,1} \rangle \end{aligned} \quad (7)$$

Since the present model (4) contains no long-range interactions in the spatial directions, $f_P(x_2)$ is expected to supply us with a good order parameter to detect a possible confinement-deconfinement transition. The deconfinement phase is characterized by small fluctuations

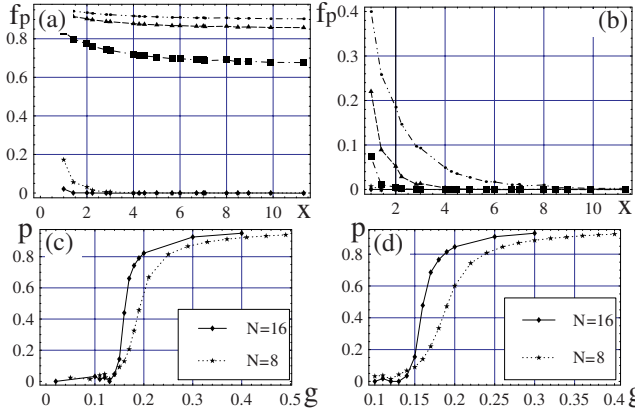


FIG. 2. Correlations of Polyakov lines, $f_p(x_2)$, vs x_2 . (a) PD ($\theta = 0, N=16$) with $g = 0.4; 0.3; 0.2; 0.1; 0.02$ from above. (b) ED ($\theta = 0, N=16$) with $g = 2.5; 2.0; 1.5; 1.0; 0.5$ from above. (c) and (d) show the order parameter $p = [f_p(x_2^{MAX})]^{1-2}$ vs g for the PD model; (c) $\theta = 0$ and (d) $\theta = 1$. They exhibit a long-range order for $g > g_c \approx 0.15$ in the PD model.

of U_x and therefore by an order in $f_p(x_2)$.

In Fig. 2, we present $f_p(x_2)$ with $\theta = 0$. The PD model of Fig. 2 (a) clearly exhibits an off-diagonal long-range order, i.e., $\lim_{x_2 \rightarrow \infty} f_p(x_2) \neq 0$ for $g > 0.20$, whereas the ED model of Fig. 2 (b) does not for all g 's. To see this explicitly, we plot in Fig. 2 (c,d) the order parameter $p = [f_p(x_2^{MAX})]^{1-2}$ for the PD model, where $x_2^{MAX} = N/2$ is the distance at which f_p becomes minimum due to the periodic boundary condition. p starts to develop continuously from zero at $g = g_c \approx 0.15$. The size dependence of p shows a typical behavior of a second-order phase transition. Thus the gauge dynamics of the PD model is realized in the deconfinement phase for $g > g_c$, whereas it is in the confinement phase for $g < g_c$. In contrast, the ED model stays always in the confinement phase. These results including the value of g_c are consistent with those derived from the data of E/C in Fig. 1.

To see the details of gauge dynamics, we measured the instanton density $\rho(x)$, an index for disorder of U_x . We employ the definition of $\rho(x)$ in U(1) LGT by DeGrand and Toussaint¹⁴. For the local 3D compact U(1) LGT without matter fields, the average density $\rho = \langle \sum_x \rho(x) \rangle / V$ is known to behave as \log / A_m if the instanton action A_m is large. The instanton gas there sustains the confinement phase even for very small A_m .

In Fig. 3 we present ρ vs g . It decreases as g increases more rapidly in the PD model than in the ED model. This behavior of ρ is consistent with the result that the PD model exhibits a second-order transition, while the ED model does not. The coupling enhances the rate of decrease in ρ as one expects since the spatial coupling favors the ordered deconfinement phase. In the ED model with $\theta = 1$, ρ is fitted by $\exp(-cg)$ with a constant c in the dilute (large g) region, and the smooth increase

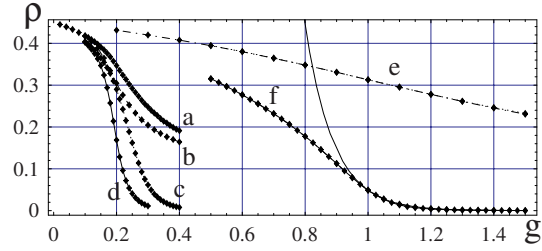


FIG. 3. Average instanton density vs g . (a) PD ($\theta = 0, N = 8$), (b) PD ($\theta = 1, N = 8$), (c) PD ($\theta = 0, N = 16$), (d) PD ($\theta = 1, N = 16$), (e) ED ($\theta = 0, N = 16$), (f) ED ($\theta = 1, N = 16$). The solid curve / $\exp(-cg)$ fits (f) at large g .

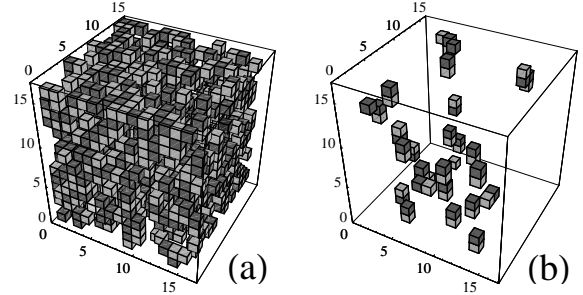


FIG. 4. Snapshots of instanton configuration $\rho(x)$ for $N=16$. (a) PD ($\theta = 1; g = 0.15$) and (b) PD ($\theta = 1; g = 0.30$). The light cubes for $\rho(x) = 1$ and the dark cubes for $\rho(x) = -1$.

for small g indicates a crossover from the dilute gas of instantons to the dense gas, just the behavior similar to the case of pure and local LGT⁶.

In Fig. 4 we show snapshots of $\rho(x)$ for the PD model with $\theta = 1$. Fig. 4 (a) is a dense gas and Fig. 4 (b) is a dilute gas. They are separated at $g_c \approx 0.20$, the location of the peak of C for $N = 16$. In Fig. 4 (b), instantons mostly appear in dipole pairs at nearest-neighbor sites, $\rho(x) = 1; \rho(x') = -1$, while in Fig. 4 (a), they appear densely and it is hard to determine their partners. In both cases, the distributions $\rho(x)$ have no apparent anisotropies like column structures. However, the orientations of dipoles in Fig. 4 (b) are mostly (92%) in the temporal direction as expected from Eq. (4).

For ordinary pure and local gauge systems, Wilson loop $W[C] = \langle \text{tr} \prod_{i \in C} U_i \rangle$ along a closed loop C on the lattice is used as an order parameter to study the gauge dynamics; $W[C]$ obeys the area law in the confinement phase and the perimeter law in the deconfinement phase;

$$W[C] \sim \begin{cases} \exp(-aS[C]); & \text{area law;} \\ \exp(-a^0L[C]); & \text{perimeter law;} \end{cases} \quad (8)$$

where $S[C]$ is the minimum area of a surface, the boundary of which is C . For a local LGT containing matter fields, $W[C]$ cannot be an order parameter because the matter fields generate the terms $\sum_C U_x$ with coefficients $\exp(-bL[C])$ in the effective action. However, in the

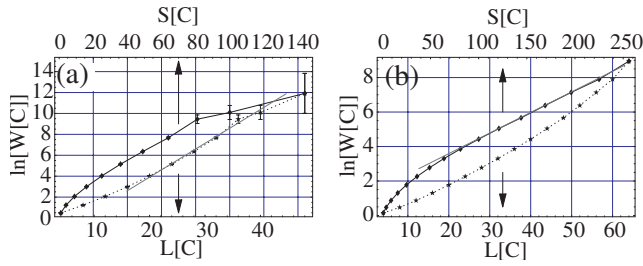


FIG. 5. Wilson loops ($N = 32$) in the 1-2 plane at large g vs L [C] or S [C]. (a) PD ($\beta = 1; g = 0.25$), (b) ED ($\beta = 1; g = 1.5$). The PD model seems to prefer the perimeter law, whereas the ED model prefers the area law.

present model (4), the nonlocal terms are restricted only along the temporal direction, so it is interesting to measure $W[C]$ for the loops lying in the spatial (1-2) plane.

In Fig. 5, we plot $W[C]$. For the PD model in Fig. 5(a), the data at $g = 0.25$ seem to prefer the perimeter law. For the ED model in Fig. 5(b), the area law fits $W[C]$ better than the perimeter law at $g = 1.5$; a considerably larger value than $g' = 1.0$ at the peak of C . This suggests the area law holds in the ED model at all g . These observations are consistent with the previous results on the (non)existence of a phase transition. Wilson loops in the spatial plane are useful to study the gauge dynamics of the present model.

We have observed that the nonlocal couplings along the temporal direction in the PD model have sufficient effect of suppressing fluctuations of U_x to produce the deconfinement phase. This result strongly suggests a deconfinement transition in the original model (2) with massless matter fields, because the isotropically distributed nonlocal couplings of the original model should have similar effect. In such a possible deconfinement phase of the original model, perturbation theory may be applicable, which predicts the potential energy between two charges as $V(r) \sim r^{-1}$, a weaker one than the 3D Coulomb potential $V(r) \sim \log(r)$.

Let us turn to the nonrelativistic case. For the t-J model, by using the hopping expansion of holons and spinons at finite T with the continuous imaginary time, we derived an effective gauge theory, which is highly nonlocal in the temporal direction. The obtained effective theory has a similar action as Eq. (4) with $c = \text{constant}$ and g/n where n is the density of matter fields (holons and spinons)⁸. The nonlocal correlations of the effective gauge field like $c = \text{constant}$ come from the fact that the nonrelativistic fermions contain a higher density of low-lying excitations compared to Dirac fermions, i.e., the existence of the Fermi surface (or line). Although the above effective gauge model is obtained for the system at finite T , we expect that a similar gauge model appears as an effective model at $T = 0$. Then it is interesting and also important to investigate the gauge model (4) with $c = \text{constant}$, the nondecaying (ND) model. The ND

model should shed some light on the anomalous normal state of cuprates because the Fermi line exists there.

We also made Monte Carlo simulation of the ND model, and obtained a phase transition similar to the PD model. However, the developing peak of C shifts to smaller g as N increases more quickly than the PD model as $g_c = 0.1$ ($N = 8$); 0.045 ($N = 16$); 0.03 ($N = 24$) for $\beta = 1$. It seems likely that $g_c \rightarrow 0$ as $N \rightarrow \infty$, that is, the deconfinement phase dominates for all $g > 0$. This may be related with the diverging coefficient Q_2 / N_0^2 in HTE, which implies that the radius of convergence is zero. This dominance of deconfinement phase of the ND model at $T = 0$ may support the CSS at finite T , which is consistent with the result of Ref.³. In contrast to the ND model, the PD model has a finite Q_2 ($= 1.645$), so has a finite region $0 < g < g_c$ of the confinement phase.

-
- ¹ J. B. Kogut and C. G. Strouthos, Phys Rev D 67, 034504 (2003) and references cited therein.
 - ² G. Baskaran and P. W. Anderson, Phys Rev B 37, 580 (1988); A. Nakamura and T. Matsui, Phys Rev B 37, 7940 (1988); D. P. Arovas and A. Auerbach, Phys Rev B 38, 316 (1988); L. B. Ioffe and A. L. Larkin, Phys Rev B 39, 8988 (1989); I. Ichinose and T. Matsui, Phys Rev B 45, 9976 (1992).
 - ³ I. A. Heck and B. Marston, Phys Rev B 37, 3774 (1988).
 - ⁴ D. Yoshioka, G. Arakawa, I. Ichinose and T. Matsui, Phys Rev B 70, 174407 (2004).
 - ⁵ I. Ichinose and T. Matsui, Phys Rev B 68, 085322 (2003) and references cited therein.
 - ⁶ A. M. Polyakov, Nucl Phys B 120, 429 (1977).
 - ⁷ P. W. Anderson, Phys Rev Lett 64, 1839 (1990).
 - ⁸ I. Ichinose and T. Matsui, Nucl Phys B 394, 281 (1993); Phys Rev B 51, 11860 (1995); Phys Rev Lett 86, 942 (2001); I. Ichinose, T. Matsui and M. Oshida, Phys Rev B 64, 104516 (2001).
 - ⁹ N. Nagaosa, Phys Rev Lett 71, 4210 (1993).
 - ¹⁰ C. Nayak, Phys Rev Lett 85, 178 (2000).
 - ¹¹ H. Kleinert, F. S. Nogueira, and A. Sudbø, Phys Rev Lett 88, 232001 (2002); Nucl Phys B 666, 361 (2003); B. B. Kirkpatrik, S. K. Raghu, and A. Sudbø, Phys Rev Lett 92, 186403 (2004); cond-mat/0412281; F. S. Nogueira and H. Kleinert, cond-mat/0501022.
 - ¹² I. F. Herbut and B. H. Seradjeh, Phys Rev Lett 91, 171601 (2003); I. F. Herbut, B. H. Seradjeh, S. Sachdev, and G. Murthy, Phys Rev B 68, 195110 (2003);
 - ¹³ For the ED case, we used Eq. (5) instead of $\exp(-m) = 1 - m$ to make the comparison with the PD case more definitive.
 - ¹⁴ T. A. DeGrand and D. Toussant, Phys Rev D 22, 2478 (1980).